Tailoring the slow light behavior in terahertz metasurfaces

Manukumara Manjappa,[1] Sher-Yi Chiam,[2] Longqing Cong,[1] Andrew A. Bettiol,[3] Weili Zhang,[4] and Ranjan Singh[1,a)]

[1]*Center for Disruptive Photonic Technologies, Division of Physics and Applied Physics, School of Physical and Mathematical Sciences, Nanyang Technological University, 21 Nanyang Link, Singapore 637371*
[2]*NUS High School of Math and Science, 20 Clementi Avenue 1, Singapore, Singapore 129957*
[3]*Department of Physics, National University of Singapore, Science Drive 3, Singapore, Singapore 117542*
[4]*School of Electrical and Computer Engineering, Oklahoma State University, 202 Engineering South, Stillwater, Oklahoma 74078, USA*

(Received 5 February 2015; accepted 20 April 2015; published online 4 May 2015)

We experimentally study the effect of near field coupling on the transmission of light in terahertz metasurfaces. Our results show that tailoring the coupling between the resonators modulates the amplitude of resulting electromagnetically induced transmission, probed under different types of asymmetries in the coupled system. Observed change in the transmission amplitude is attributed to the change in the amount of destructive interference between the resonators in the vicinity of strong near field coupling. We employ a two-particle model to theoretically study the influence of the coupling between bright and quasi-dark modes on the transmission properties of the system and we find an excellent agreement with our observed results. Adding to the enhanced transmission characteristics, our results provide a deeper insight into the metamaterial analogues of atomic electromagnetically induced transparency and offer an approach to engineer slow light devices, broadband filters, and attenuators at terahertz frequencies. © *2015 AIP Publishing LLC*.
[http://dx.doi.org/10.1063/1.4919531]

Light-matter interaction has been a subject of intense research over past several decades, since it allows to probe the resonance and the off-resonance properties of the materials over large part of the electromagnetic spectrum. Until late twentieth century, light-matter interaction in the terahertz part of the electromagnetic spectrum was the least explored. With the advent of metamaterials,[1] which exhibit structure dependent resonance properties, have become excellent candidates for probing such resonant and off-resonant interactions at terahertz frequencies. Metamaterials are composed of periodic array of sub wavelength sized meta-atoms, which exhibit strong near-field coupling that can carry the interaction energy over to the far field regimes. Superlens,[2,3] polarization independent negative refraction,[4] hybridization,[5,6] Fano-coupling,[7] and the classical analogue of electromagnetically induced transparency (EIT)[8–12] have been studied and demonstrated using the near field coupling within the metamaterials. Recently, there have been a enormous interest in the near-field coupling in terahertz metamaterials, which show EIT like transmission[11–13] and ultra high Q Fano[14] and even eigenmode resonances,[15] which find significant applications in the terahertz sensing[16] and broadband communication technologies.[17]

Electromagnetically induced transparency is a quantum interference effect, which was first observed[18] in a three level atomic system, owing to the destructive interference between the possible excitation pathways. Later, its analogue was extended to the classical systems,[19] since then EIT like effects have been observed in various classical systems, including metamaterials,[8–13] photonic crystals,[20] micro ring resonators,[21,22] and all dielectric metasurfaces.[23] There have been a few reports on tailoring the classical analogue of EIT using metamaterials at microwave,[24,25] terahertz,[26–28] and optical frequencies,[8,29] either by tuning the near field coupling or by changing the material properties. Manipulation of EIT in classical systems will allow us to precisely tailor the group velocity[30,31] and the delay bandwidth product[24] of the transmitted pulse. Moreover, it provides a clear picture of the coupling mechanisms in the classical analogue of EIT, which can help us in drawing the closest analogy between the classical and the quantum systems. In this letter, we experimentally demonstrate the enhancement and suppression in transmission of the light at terahertz frequencies, by manipulating the near field coupling between the radiative dipole ring (CRR) and the sub-radiant quasi-dark split ring resonator (SRR) in metasurfaces under different type of asymmetries of the metamolecule. Systems with enhanced transmission show a considerable increase in the delay bandwidth product (DBP) at the transmission peak.

Metamaterial unit cells (Fig. 1) consist of a metallic SRR surrounded by a concentric metallic closed square ring resonator (CRR), both having a thickness of 200 nm. Samples were fabricated using photolithography technique, where 200 nm thin layer of aluminium is deposited on 640 μm thick n-type silicon substrate ($\epsilon = 11.68$). Structural symmetry of the metamolecule unit cells were broken to study the impact of the near field coupling in the asymmetric metasurface array. For the metasurfaces (MS-3 and MS-4) with SRR-gap asymmetry, the capacitive split gap in the SRR of MS-1 and MS-2 is displaced horizontally (along the x-axis) by 5 μm from the y-symmetry axis, whereas for the metasurfaces with SRR-position asymmetry (MS-2 and MS-4), position of the inner SRR in MS-1 and MS-3 is displaced upwards (along the y-axis) by 4 μm from the x-symmetry

a)Electronic mail: ranjans@ntu.edu.sg

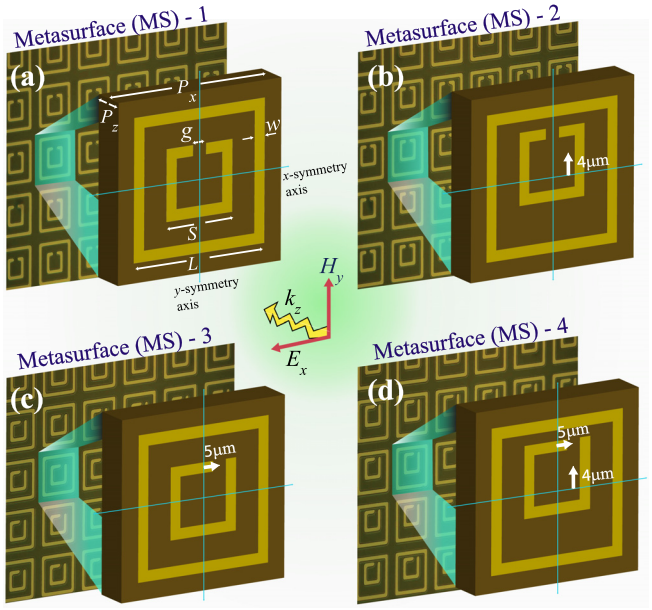

FIG. 1. Metasurfaces showing (a) symmetry (MS-1), (b) SRR-position asymmetry (MS-2), (c) SRR-gap asymmetry (MS-3), and (d) SRR-position and SRR-gap asymmetry (MS-4) are graphically displayed. In the case of (b) and (d), SRR ring is displaced upwards by 4μm from the x-symmetry axis, whereas in (c) and (d) SRR gap is displaced sidewards by 5 μm from the y-symmetry axis. All four metasurface samples have same material dimension: L, 40 μm; S, 20 μm; g, 4 μm; w, 3 μm; periodicity (P_x) of the unit cell is 50 μm with substrate thickness (P_z) of 640 μm.

axis (see Fig. 1). The design of each metamolecule was chosen such that the fundamental resonance frequencies of their constituent resonators, exhibiting highly contrasting resonance linewidths, fall at the same frequency, which is essential to realize the EIT like behavior in classical systems. Fig. 2(a) depicts the contrasting resonance linewidths for the CRR and the SRRs. The CRR gives a broad dipolar resonance and the nature of near-field coupling in such metamaterial structures has been probed in detail in Ref. 4. The measured Q-factor for CRR is 1.2, which is an order of magnitude lower than that of the Q-factor of inner SRR. For the symmetric SRR, the Q-factor is 10.6, whereas the asymmetric SRR (SRR with displaced gap) has a Q-factor of 11.3.

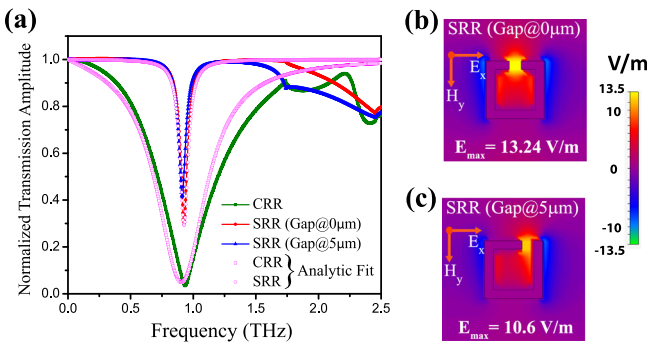

FIG. 2. (a) Graph displaying the individual resonance dips for the outer closed ring resonator (CRR) (green squares), the symmetric SRR (red circles), and the asymmetric SRR (blue triangles) along with analytic fit to the CRR and SRR resonances are shown in magenta squares and circles, respectively. Electric field strengths for the symmetric (b) and the asymmetric (c) SRR rings are also shown.

Here, we would like to stress that both the resonators, CRR and the SRR interact with the incoming electric field (E_x), but with different coupling strengths. In the uncoupled case, the relative coupling of the CRR and the SRR with the incoming field is quantitatively given by Eqs. (1) and (2) (for $\Omega = 0$), respectively. From the analytic fit (Fig. 2(a)), the estimated coupling strength of CRR to the incoming radiation (E_x) is "twice" stronger than the coupling strength of the SRR. Thus, the strongly coupled CRR with broad dipolar resonance (lower Q-factor) behaves like a "bright mode," where as the weakly coupled SRR with sharp LC resonance (higher Q-factor) is termed as "quasi-dark mode."

Figures 3(a)–3(d) show the sharp transmission spectra for each of the metamaterial samples. Spectra were recorded using 8f confocal terahertz time domain spectroscopy (THz-TDS) for the incident electric field (E_x), polarized along the gap (x-axis) of the SRR. Recorded transmission time domain signals were converted to frequency domain data using FFT and normalized to the transmission of the bare silicon substrate (as reference). Corresponding numerical simulations were carried out using the commercially available CST MICROWAVE STUDIO Maxwell equation solver and the data matched well with our measured results (insets of Fig. 3).

Fig. 3(a) depicts EIT like transmission spectrum for MS-1, where, between two transmission dips a sharp transmission peak is observed at the frequency 0.88 THz, which signifies the hybridization model of the plasmonic coupling via near fields of the individual resonators. This behaviour is verified by simulating the surface current distribution as shown in Fig. 4(a) for MS-1, where at the transmission dips ((i) and (iii)), surface currents in the SRR and the CRR run antiparallel and parallel to each other, respectively, for the (i) antisymmetric and the (iii) symmetric modes. Existence of the antisymmetric mode at the lower frequency signifies strong transverse dipole-dipole interaction within the coupled system. On the other hand, at the (ii) transparency peak, the induced surface current appears to be localized within the SRR of the coupled system, which implies that the field in the SRR will have an influence on the CRR by their near field coupling.

Introducing SRR-gap asymmetry in the system (MS-3) leads to a suppression in the transmission amplitude of the resulting transparency peak (Fig. 3(c)). This suppression is solely due to the weakened SRR resonance (refer blue curve in Fig. 2(a)), because of its structural asymmetry. Displacing the gap to one end of the SRR arm results in rather a flaccid and weak electric field distribution (Fig. 2(c)) at the SRR gap. This weakens the capacitive coupling within the SRR ring. As a result, the effective strength of the quasi-dark mode (SRR) decreases and results in a reduced transmission. Owing to the interference effects in EIT phenomenon, this result can be seen as analogous to the waves' interference, where decreasing the amplitude of one of the wave results in the decreased strength of interference pattern. The same explanation holds true for the observed suppression in the transmission for MS-4 (Fig. 3(d)) compared with the transmission of MS-2 (Fig. 3(b)).

Upon introducing SRR-position asymmetry in the system, transmission through MS-2(4) shows an enhancement over the transmission observed for MS-1(3), as shown in

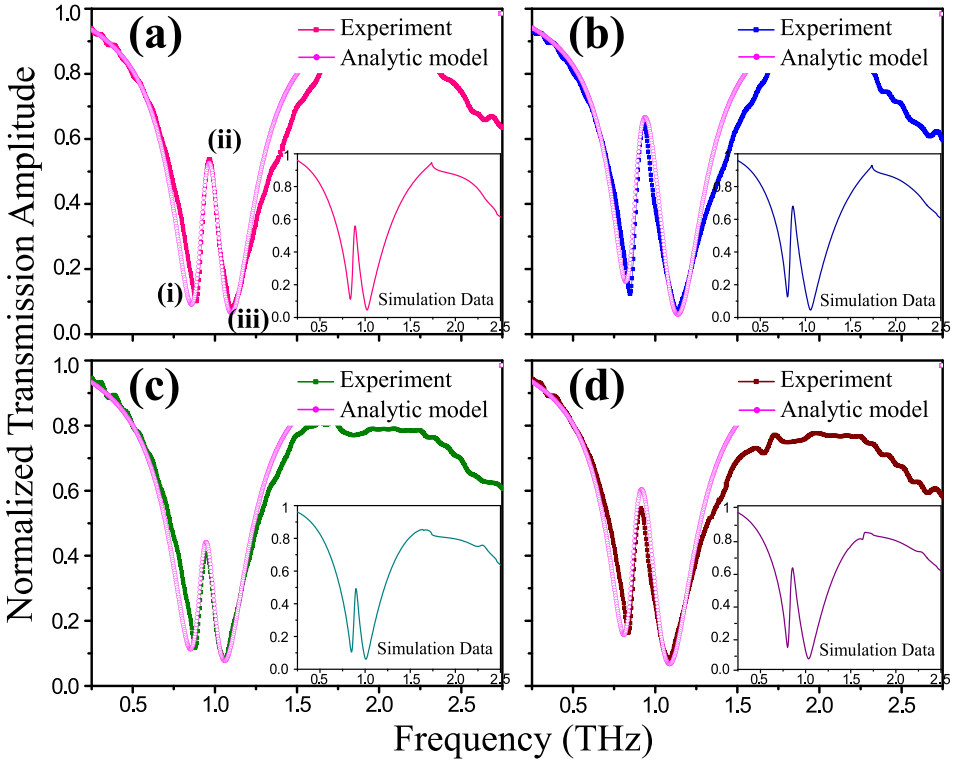

FIG. 3. Terahertz transmission spectra for the incident E_x field. (a)–(d) The experimentally measured as well as simulated transmission (inset) curves for metasurface samples MS-1, MS-2, MS-3, and MS-4, respectively. Experimentally measured transmission curves are fitted with corresponding analytic model data (colored magenta). (i), (ii), and (iii) in (a), simultaneously represents the antisymmetric, transmission, and symmetric modes of the plasmonic hybridization, which is detailed in Fig. 4(a).

Figs. 3(b) and 3(d). Enhanced transmission is due to increased coupling between the CRR and the SRR,[32] which results in strong destructive interference of the two fields at the transmission peak. This effect can be explained using Fig. 4(c), which depicts the change in the strength of induced surface currents at the transparency peaks, for all the four coupled metasuface structures. For MS-1(3), strongly confined field in the SRR induces opposing image currents in CRR, which results in a destructive interference of the fields, giving rise to a sharp transmission peak. As the SRR gap (stronger E-field confinement) comes closer to the bright mode (top arm of the CRR), electric coupling between the two modes dominates the interaction. This enhances the effective coupling in the system that leads to a strong cancellation of the opposing currents (enhanced destructive interference) within the coupled modes, resulting in an increased transmission of the incident field. This effect is also reflected in the E-field distribution diagram as shown in Fig. 4(b), where at the transparency peak for the metasurfaces MS-2 and MS-4, the E-field in the coupled system is decreased (compared with MS-1 and MS-2) as the result of the enhanced destructive interference between the two modes. Thus, the entire system behaves as super-radiative system with smaller Q-value. On the other hand, the inverse situation holds true, when the SRR ring is displaced downwards, which reduces the destructive interference within the system that results in decreased transmission. The observed frequency red shift of the transmission peak and the antisymmetric mode for the MS-2 and MS-4 (see Fig. 3), indicates the increased electric field strength within the coupled metamaterial system. Thus, by moving the quasi-dark mode relative to the bright mode, we can tailor the electromagnetically induced transparency by changing the coupling strength within the system.

Effect of coupling on the transmission of light in the coupled metamaterial system is theoretically studied using the Lagrangian,[33] and two particle model[25] to describe the effective coupling in the system. The former one probes the individual strengths of electric and magnetic dipoles in SRRs, whereas the latter one considers effective coupling in the system. Here, we employ two particle model, where we consider both particles (bright (x_b) and quasi-dark (x_d)) interact with the incoming electric field $E = E_0 e^{i\omega t}$

$$\ddot{x}_b(t) + \gamma_b \dot{x}_b(t) + \omega_b^2 x_b(t) + \Omega^2 x_d(t) = \frac{QE}{M}, \tag{1}$$

$$\ddot{x}_d(t) + \gamma_d \dot{x}_d(t) + \omega_d^2 x_d(t) + \Omega^2 x_b(t) = \frac{q_d E}{m_d}. \tag{2}$$

Here, (Q, q_d), (M, m_d), (ω_b, ω_d), and (γ_b, γ_d) are the effective charge, effective mass, resonance angular frequencies, and the loss factors of the bright and the quasi-dark modes, respectively. Ω defines the coupling strength between the bright and quasi-dark particles. In the above coupled equations, we substitute $q_d = \frac{Q}{A}$ and $m_d = \frac{M}{B}$, where A and B are dimensionless constants that dictate the relative coupling of incoming radiation with the bright and the quasi-dark modes. Now by expressing the displacements vectors for bright and quasi-dark modes as $x_b = c_b e^{i\omega t}$ and $x_d = c_d e^{i\omega t}$, we solve the above coupled equations (1) and (2) for x_b and x_d

$$x_b = \frac{\left((B/A)\Omega^2 + \left(\omega^2 - \omega_d^2 + i\omega\gamma_d\right)\right)(QE/M)}{\Omega^4 - \left(\omega^2 - \omega_b^2 + i\omega\gamma_b\right)\left(\omega^2 - \omega_d^2 + i\omega\gamma_d\right)} \tag{3}$$

and

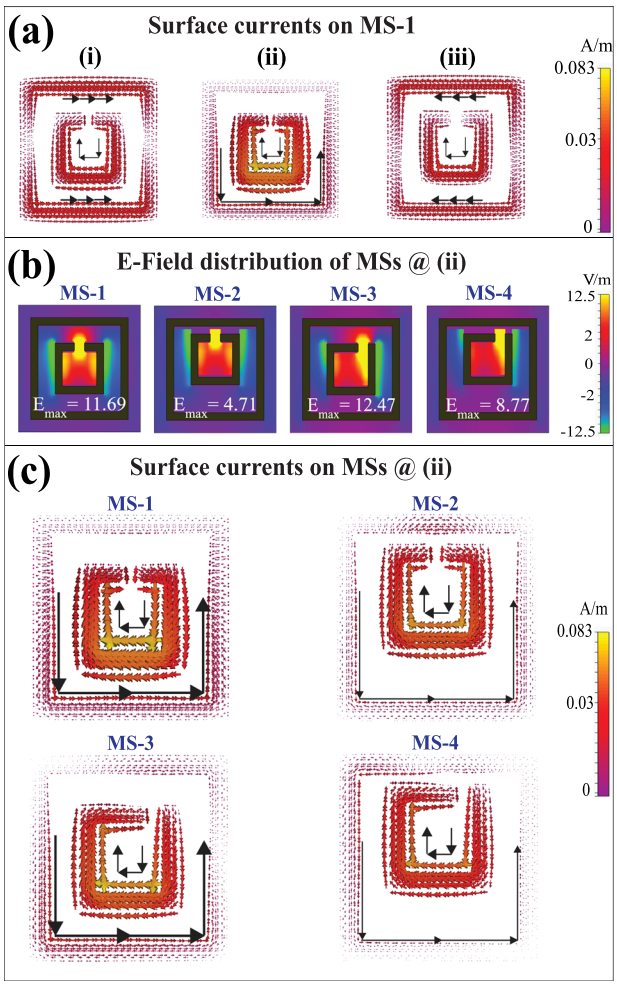

FIG. 4. (a) Induced surface currents within the hybridized system at transmission dips ((i) 0.83THz and (iii) 1.02THz) and at the transmission peak ((ii) 0.88THz) for the metasurface MS-1, are shown. (b) E_x-field distribution at the transmission peak (ii) is shown for each metasurface samples. (c) Depicts the surface current distributions for the metasurfaces MS-1, MS-2, MS-3, and MS-4 at their respective transmission peaks.

$$x_d = \frac{\left(\Omega^2 + (B/A)\left(\omega^2 - \omega_b^2 + i\omega\gamma_b\right)\right)(QE/M)}{\Omega^4 - \left(\omega^2 - \omega_b^2 + i\omega\gamma_b\right)\left(\omega^2 - \omega_d^2 + i\omega\gamma_d\right)}. \quad (4)$$

The linear susceptibility (χ), which relates the polarization (P) of the particle to the strength of incoming electric field (E) is expressed in terms of the displacement vectors as, $\chi = \frac{P}{\epsilon_0 E} = \frac{Qx_b + q_d x_d}{\epsilon_0 E}$

$$\chi = \frac{K}{A^2 B}\left(\frac{A(B+1)\Omega^2 + A^2\left(\omega^2 - \omega_d^2\right) + B\left(\omega^2 - \omega_b^2\right)}{\Omega^4 - \left(\omega^2 - \omega_b^2 + i\omega\gamma_b\right)\left(\omega^2 - \omega_d^2 + i\omega\gamma_d\right)} + i\omega\frac{A^2\gamma_d + B\gamma_b}{\Omega^4 - \left(\omega^2 - \omega_b^2 + i\omega\gamma_b\right)\left(\omega^2 - \omega_d^2 + i\omega\gamma_d\right)}\right). \quad (5)$$

Here, Re[χ] represents the dispersion and Im[χ] gives the absorption (loss) within the medium. We fit $1 - \text{Im}[\chi]$, to the experimental data shown in Fig. 3 (colored magenta), which represents the transmission through a medium. For the fit, the values of the loss factors γ_b and γ_d are obtained from the linewidths of the curves shown in Fig. 2(a), which are calculated to be around 3×10^{12} rad/s and 5×10^{11} rad/s, respectively. The coupling strength Ω for each transmission curves is calculated using the formula given in Ref. 25, which can also be derived from Eq. (5) at the stop-band frequencies $\omega_\pm$, for a loss less medium (assuming ω_b, $\omega_d = \omega_0$). Using Eq. (5), at the transparency peak ($\omega = \omega_T$) where $\text{Re}[\chi] = 0$, we get, $\omega_d \approx \omega_T$ for larger A. At the stop-bands where $\text{Im}[\chi] = \infty$, by using Eq. (5) we can arrive at the expression for ω_b (assuming $\omega_d = \omega_T$), $\omega_{b\pm} = \sqrt{\omega_\pm^2 \mp \frac{\Omega^4}{\Omega_\pm^2}}$. By substituting the calculated values for γ_b, γ_d, ω_b, ω_d, and Ω and by putting $B = 2$ (mass of SRR is half the mass of CRR) and $K = 4 \times 10^{25}$ (amplitude offset) in Eq. (5), we find an excellent fit for the transmission curves shown in Fig. 3, for parameter $A = 40$. This suggests that, within these coupled metamaterial systems, interaction of the bright mode to the incoming radiation is nearly "20 times" stronger than that of the quasi-dark mode. We have shown that, besides providing the closest analogy to the observed results for the current system under consideration, the proposed model gives an estimation of the relative coupling of the bright and the quasi-dark modes to the incoming radiation in the uncoupled and the coupled situations. To further evaluate coupling effects in these systems, we study the influence of coupling strength (Ω) on the Q-factors of the transmission curves. We find that the Q-factors obtained from the simulated transmission curves for the samples with different SRR positions (SRR-position asymmetries) follow $\frac{K}{\Omega^2}$ variation (Fig. 5(a)), as predicted by the two particle model.[25]

Figure 5(b) shows a variation of the measured group delay values for the transmission curves given in Fig. 3. Experimentally measured values for group delay, DBP, and the respective Q-factors for the transmission curves for all

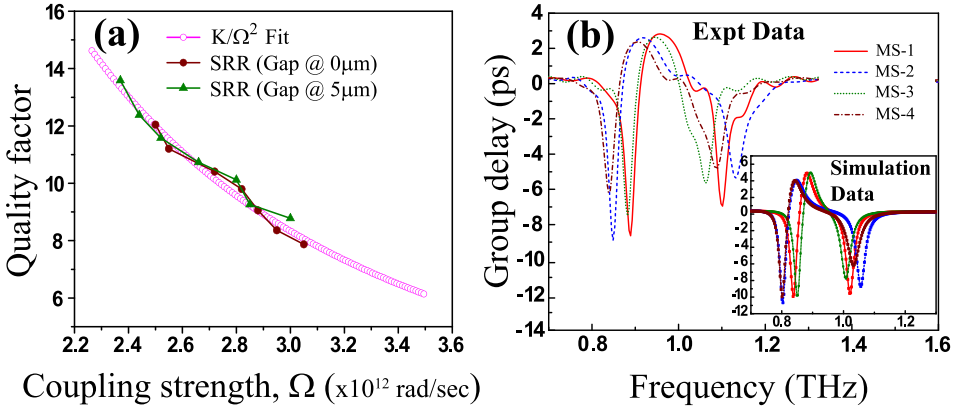

FIG. 5. (a) K/Ω^2 fit to the variation of Q-factors of the transmission curves with the coupling strength Ω, under various SRR-position asymmetries of the metasurface samples. Brown curve represents Q-factor variation for metasurfaces with symmetric SRR ring, and green curve represents metasurfaces with asymmetric SRR ring. (b) Both experimental and simulated group delay data for the incident radiation within the transparency peak.

TABLE I. Calculated group delay, DBP, and Q-factor values for the experimentally measured transmission curves shown in Fig. 3.

Metasurface Samples (MSs)	Group delay $t_g = \frac{-d\phi}{d\omega}$ (ps)	DBP $(t_g \times \Delta f)$	Q-factor
MS-1	2.77	0.21	11.74
MS-2	2.52	0.217	9.83
MS-3	2.63	0.174	13.35
MS-4	2.35	0.18	11

the four metasurface samples are listed in Table I. From the data we see that as coupling increases, DBP increases and the corresponding Q-factor decreases and vice versa. For example, MS-2 that displays stronger mode coupling compared to all other samples, possesses maximum DBP and minimum Q-factor.

In summary, we have demonstrated that by introducing SRR-gap asymmetry in the system suppresses the transmission, whereas the system with SRR-position asymmetry results in enhanced transmission due to increased coupling strength. Our results clearly show that the resulted transmission is due to the destructive interference between the fields of the two resonators, which is the essence of the EIT like phenomenona in classical systems. This study provides a deeper insight into the classical analogy of the quantum interference effect arising in the three level atomic EIT systems. The proposed asymmetric planar slow light metasurfaces with tunable transparency characteristics will allow us to precisely control the group velocity of the pulse within the medium. They can be readily applied in broadband terahertz technologies and show potential applications as variable power attenuators, broadband filters, and compact delay lines for the terahertz waves.

The authors thank Andal Narayanan, D Wilkowski, and the anonymous referee for their helpful and constructive comments. M.M, L.C., and R.S. acknowledge the financial support from NTU startup Grant No. M4081282 and MoE Tier 1 Grant No. M4011362.

[1]J. B. Pendry, A. J. Holden, D. J. Robbins, and W. J. Stewart, IEEE Trans. Microwave Theory Tech. **47**, 2075 (1999); D. R. Smith, W. J. Padilla, D. C. Vier, S. C. Nemat-Nasser, and S. Schultz, Phys. Rev. Lett. **84**(18), 4184 (2000).
[2]J. B. Pendry, Phys. Rev. Lett. **85**, 3966 (2000).
[3]N. Fang, H. Lee, C. Sun, and X. Zhang, Science **308**, 534–538 (2005).
[4]B. Kanté, Y.-S. Park, K. O'Brien, D. Shuldman, N. D. Lanzillotti Kimura, Z. Jing Wong, X. Yin, and X. Zhang, Nat. Commun. **3**, 1180 (2012).
[5]E. Prodan, C. Radloff, N. J. Halas, and P. Nordlander, Science **302**, 419–422 (2003).
[6]N. Liu, S. Kaiser, and H. Giessen, Adv. Mater. **20**, 4521–4525 (2008).
[7]B. Luk'yanchuk, N. I. Zheludev, S. A. Maier, N. J. Halas, P. Nordlander, H. Giessen, and C. Tow Chong, Nat. Mater. **9**, 707–715 (2010).
[8]S. Zhang, D. A. Genov, Y. Wang, M. Liu, and X. Zhang, Phys. Rev. Lett. **101**, 047401 (2008).
[9]N. Papasimakis, V. A. Fedotov, and N. I. Zheludev, Phys. Rev. Lett. **101**, 253903 (2008).
[10]V. Yannopapas, E. Paspalakis, and N. V. Vitanov, Phys. Rev. B **80**, 035104 (2009).
[11]R. Singh, C. Rockstuhl, F. Lederer, and W. Zhang, Phys. Rev. B **79**, 085111 (2009).
[12]S.-Y. Chiam, R. Singh, C. Rockstuhl, F. Lederer, W. Zhang, and A. A. Bettiol, Phys. Rev. B **80**, 153103 (2009); W. Cao, R. Singh, C. Zhang, J. Han, M. Tonouchi, and W. Zhang, Appl. Phys. Lett. **103**(10), 101106 (2013).
[13]R. Singh, I. Al-Naib, D. R. Chowdhury, L. Cong, C. Rockstuhl, and W. Zhang, Appl. Phys. Lett. **105**, 081108 (2014).
[14]W. Cao, R. Singh, I. A. I Al-Naib, M. He, A. Taylor, and W. Zhang, Optics Letters **37**, 3366 (2012); R. Singh, I. Al-Naib, W. Cao, C. Rockstuhl, M. Koch, and W. Zhang, IEEE Trans. Terahetz Sci. Technol. **3**, 820 (2013).
[15]I. Al-Naib, Y. Yang, M. M. Dignam, W. Zhang, and R. Singh, Appl. Phys. Lett. **106**, 011102 (2015).
[16]R. Singh, W. Cao, I. Al-Naib, L. Cong, W. Withayachumnankul, and W. Zhang, Appl. Phys. Lett. **105**, 171101 (2014).
[17]N. Papasimakis and N. I. Zheludev, Opt. Photonics News **20**, 22 (2009).
[18]K.-J. Boller, A. Imamoğlu, and S. E. Harris, Phys. Rev. Lett. **66**, 2593 (1991).
[19]C. L. Garrido Alzar, M. A. G. Martinez, and P. Nussenzveig, Am. J. Phys. **70**(1), 37 (2002).
[20]M. F. Yanik, W. Suh, Z. Wang, and S. Fan, Phys. Rev. Lett. **93**, 233903 (2004).
[21]D. D. Smith, H. Chang, K. A. Fuller, A. T. Rosenberger, and R. W. Boyd, Phys. Rev. A **69**, 063804 (2004).
[22]Q. Xu, S. Sandhu, M. L. Povinelli, J. Shakya, S. Fan, and M. Lipson, Phys. Rev. Lett. **96**, 123901 (2006).
[23]Y. Yang, I. I. Kravchenko, D. P. Briggs, and J. Valentine, Nat. Commun. **5**, 5753 (2014).
[24]Y. Sun, H. Jiang, Y. Yang, Y. Zhang, H. Chen, and S. Zhu, Phys. Rev. B **83**, 195140 (2011).
[25]F.-Y. Meng, Q. Wu, D. Erni, K. Wu, and J.-C. Lee, IEEE Trans. Microwave Theory Tech. **60**, 3013 (2012).
[26]S. Han, R. Singh, L. Cong, and H. Yang, J. Phys. D: Appl. Phys. **48**, 035104 (2015).
[27]X. Liu, J. Gu, R. Singh, Y. Ma, J. Zhu, Z. Tian, M. He, J. Han, and W. Zhang, Appl. Phys. Lett. **100**, 131101 (2012).
[28]X. Yin, T. Feng, S. Yip, Z. Liang, A. Hui, J. C. Ho, and J. Li, Appl. Phys. Lett. **103**, 021115 (2013).
[29]N. Liu, L. Langguth, T. Weiss, J. Kästel, M. Fleischhauer, T. Pfau, and H. Giessen, Nat. Mater. **8**, 758 (2009).
[30]J. Gu, R. Singh, X. Liu, X. Zhang, Y. Ma, S. Zhang, S. A. Maier, Z. Tian, A. K. Azad, H.-T. Chen, A. J. Taylor, J. Han, and W. Zhang, Nat. Commun. **3**, 1151 (2012).
[31]F. Miyamaru, H. Morita, Y. Nishiyama, T. Nishida, T. Nakanishi, M. Kitano, and M. W. Takeda, Sci. Rep. **4**, 4346 (2014).
[32]G. R. Keiser, H. R. Seren, A. C. Strikwerda, X. Zhang, and R. D. Averitt, Appl. Phys. Lett. **105**, 081112 (2014).
[33]D. A. Powell, M. Lapine, M. V. Gorkunov, I. V. Shadrivov, and Y. S. Kivshar, Phys. Rev. B **82**, 155128 (2010).